PHYSICAL REVIEW A **76**, 042702 (2007)

Wave-packet approach to Rydberg resonances in dissociative recombination

Sabine Morisset[*]
Laboratoire des Interactions Ioniques et Moléculaires, Université de Provence - Centre National de la Recherche Scientifique,
Centre Saint-Jérôme, Equipe SdM, Service 242, 13397 Marseille cedex 20, France

Lukáš Pichl[†]
Max Planck Institute for the Physics of Complex Systems, Nöthnitzer Straße 38, D-01187 Dresden, Germany

Ann E. Orel[‡]
Department of Applied Science, University of California, Davis, California 95616, USA

Ioan F. Schneider[§]
Laboratoire de Mécanique, Physique et Géosciences, Unité de Formation et de Recherche Sciences et Techniques, Université du Havre,
25, rue Philippe Lebon, BP 540, 76058, Le Havre, France

(Received 22 March 2007; published 2 October 2007)

We report the time-dependent approach to resonant electron capture into Rydberg states in collisions with molecular cations at low impact energy, as an alternative to the method based on multichannel quantum defect theory (MQDT), and present the results for the HD$^+$ ion. The propagation of the initial wave function on 13 Rydberg states (besides one valence state) correctly describes the *indirect* dissociative recombination mechanism in the time domain. Notably, the *nonlocal* coupling operator between the ionization and dissociation channels is accounted for in the *indirect* process, extending previous work on the case of direct coupling. The present approach compares to the MQDT framework with remarkable precision: resonant structures in the cross section correctly emerge from the wave-packet propagation; the time-dependent result also forms a cross section envelope for the dense series of ultrafine MQDT resonances corresponding to the quasicontinuous part of the Rydberg state manifold.

DOI: 10.1103/PhysRevA.76.042702 PACS number(s): 34.80.Ht, 34.80.Lx, 34.80.Kw

I. INTRODUCTION

In the interstellar molecular clouds, in the planetary ionospheres, in the devices of combustion, de-pollution, material processing (conventional or plasma-assisted), and close to the walls of the controlled fusion reactors, dissociative recombination (DR) [1] resulting from the collisions of electrons and molecular cations (charge recombination accompanied by fragmentation) is one of the key processes mediating energy exchange and chemical balance. Consequently, the DR is an active area of research [2–6].

Most of the experiments devoted to DR in a broad range of energy have been performed in magnetic and electrostatic storage rings of heavy ions in Heidelberg, Stockholm, Aarhus, and Tokyo [7,8]. On the other hand, plasma-type experiments based on the flowing afterglow Langmuir probe (FALP) technique provided numerous thermal rates [9].

On the theoretical side, the multichannel quantum defect theory (MQDT) [10–19], the R-matrix method [20], and the wave-packet method [21–23] have been employed. Since DR involves interaction of dissociation and ionization continua, we should notice here that the time-dependent technique has been already employed within a generalized MQDT, in the study of predissociation and of preionization [24].

For many years, the MQDT proved to be efficient in accurately representing the numerous resonances in the DR cross section structure, related to temporary captures into highly excited Rydberg states, but unable to describe the origin of branching ratios for output products, a consequence of a fixed frame transform between the inner and outer coordinate space regions. This issue was successfully addressed by using the wave-packet method [23], however, without accounting in detail for the resonant capture at low energy.

This work completes in the latter aspect the series of the wave-packet studies, and provides *low* energy (i.e., below the ion dissociation threshold) wave-packet-computed cross sections for the benchmark HD$^+$ DR reaction. This approach is motivated by the configuration interaction formulation of channel interactions in DR, performed by Giusti-Suzor *et al.* [12] two decades ago, and further by the dualism of the time-dependent and time-independent frameworks expressed via the application of Fourier transform technique [25,26], which has also been employed by Orel and co-workers in recent DR calculations [21,23].

II. METHOD

Briefly, the eigenfunction $\Psi(q,R,E)$ of the total molecular Hamiltonian is expanded in terms of Born-Oppenheimer products corresponding to the relevant configurations,

---

[*] Formerly at Laboratoire de Mécanique, Physique et Géosciences, Université du Havre. sabine.morisset@univ-provence.fr

[†] On summer leave from International Christian University, Tokyo. lukas@icu.ac.jp

[‡] aeorel@ucdavis.edu

[§] ioan.schneider@univ-lehavre.fr

©2007 The American Physical Society

$$\Psi(q,R,E) = \int_{-\infty}^{+\infty} d\mathcal{E} \sum_{\nu} [b_\nu(\mathcal{E},E)\psi_{\nu\mathcal{E}}(q,R) + b'_\nu(\mathcal{E},E)\psi'_{\nu\mathcal{E}}(q,R)]\chi_\nu(R) + \phi_d(q,R)\zeta_d(R,E) + \sum_p \psi_p(q,R)\zeta_{Ryd,p}(R,E) + \sum_{p'} \psi'_{p'}(q,R)\zeta'_{Ryd,p'}(R,E). \qquad (1)$$

In the above formula, q and R label the electronic and internuclear coordinates, respectively, E is the total energy of the molecular system, and $\mathcal{E}$ stands for the total energy of the ionization continuum. The vibrational quantum number of the target molecular ion is denoted by ν, while p and p' are the electronic quantum numbers of the Rydberg states of the neutral molecule.

This expansion relates to Eq. (4) from [12], but has been modified for the case of HD$^+$ in two respects. First, there are two electron-ion continua, $\psi_{\nu\mathcal{E}}$ and $\psi'_{\nu\mathcal{E}}$, as compared to one continuum in Ref. [12]. For the HD system, this corresponds to the s and d partial waves of the electron in continuum associated with the $X^2\Sigma_g^+$ ground state ionic configuration, which interacts effectively with the dissociative electronic state ${}^1\Sigma_g^+\ (2p\sigma_u)^2$.

The integral over the "electron+ion" continua is extrapolated [12] below the ionization threshold to the sums on the corresponding Rydberg ψ_p and $\psi'_{p'}$ states but, as the second modification, the products between energy-dependent *coefficients* and vibrational wave functions of the Rydberg states have been replaced by general *functions* $\zeta_{Ryd,p}(R,E)$ and $\zeta'_{Ryd,p'}(R,E)$ to be determined. Together with these two functions, the energy-dependent coefficients $b_\nu(\mathcal{E},E)$ and $b'_\nu(\mathcal{E},E)$, and $\zeta_d(R,E)$ [the multiplicative amplitude of the dissociative electronic state $\phi_d(q,R)$] should be evaluated in order to obtain the DR cross section. Successive projections of the Schrődinger equation on the expansion functions $\psi_{\nu\mathcal{E}}$, ϕ_d, and ψ_p yield

$$\begin{bmatrix} T_R + E_d - E & \rho_1 V_{el} & \rho'_1 V'_{el} & \cdots & \rho'_n V'_{el} \\ \rho_1 V_{el} & T_R + U_1 - E & 0 & \cdots & 0 \\ \rho'_1 V'_{el} & 0 & \cdot & \cdot & 0 \\ \vdots & \vdots & \cdot & \cdot & \vdots \\ \rho'_n V'_{el} & 0 & 0 & \cdots & T_R + U'_n - E \end{bmatrix} \begin{pmatrix} \zeta_d \\ \zeta_{Ryd,1} \\ \vdots \\ \zeta_{Ryd,n} \\ \zeta'_{Ryd,n} \end{pmatrix} = \begin{pmatrix} -(V_{el} + V'_{el})\chi_{\nu_i} + i\pi \sum_\nu (V_{el} d_\nu + V'_{el} d'_\nu)\chi_\nu \\ 0 \\ \cdot \\ \cdot \\ 0 \end{pmatrix}, \qquad (2)$$

where T_R is the relative internuclear kinetic energy operator, $E_d(R)$ is the energy of the dissociative (valence) state, $U_1(R)$, $U'_1(R), \ldots, U'_n(R)$ denote the electronic energies of the Rydberg states, ρ_1, $\rho'_1, \ldots, \rho'_n$ stand for the corresponding density of states, and finally $V_{el}(R)$ and $V'_{el}(R)$ are the couplings between the ionization continua and the dissociation one [12]. The *nonlocal* [21] term depends on $\zeta_d(R,E)$ via the occurrence of $d_\nu(E)$,

$$d_\nu(E) = \langle \chi_\nu(R) | V_{el}(R) | \zeta_d(R,E) \rangle. \qquad (3)$$

Following the technique already used to implement the so-called "boomerang model" into a time-dependent context [25,26], we build a *time-dependent* system equivalent to Eq. (2) by means of the Fourier transform. In this case, Eq. (2) is modified in the following way: E is replaced by $i\hbar\frac{\partial}{\partial t}$, the internuclear wave functions $\zeta_d(R,E)$, $\zeta_{Ryd_1}(R,E)$, etc. are replaced respectively by their Fourier transform in time $\zeta_d(R,t)$, $\zeta_{Ryd_1}(R,t)$, and so forth. Within this time-dependent framework, and in analogy to previous studies [21,23], the task is to propagate a wave packet initially localized on the vibrational state of the target ion ν_i,

$$\zeta_d(R,t=0) = [V_{el}(R) + V'_{el}(R)]\chi_{\nu i}(R), \qquad (4)$$

through the valence and Rydberg potential energy curves simultaneously. Let us note that initially the Rydberg states are not populated. The DR cross section is obtained as in [21], after projecting the corresponding long-time propagated wave packet on the plane wave associated with the final fragments,

$$\sigma = g\frac{\pi^2 m}{\varepsilon k}\left| \lim_{t\to\infty}\left[\int_0^\infty e^{-ikR}\zeta_d(t,R)dR \right] \right|^2, \qquad (5)$$

where ε is the energy of the incident electron, m is the reduced mass of the nuclei, and k the wave number corresponding to the dissociation kinetic-energy release.

The wave-packet propagation for results presented in this work was performed simultaneously on the valence state $(2p\sigma_u)^2\ {}^1\Sigma_g^+$ and on 13 Rydberg states $(1s\sigma_g nl\sigma_g)\ {}^1\Sigma_g^+$, l=0, 2 displayed in Fig. 1. In order to solve the matrix time-dependent version of Eq. (2), we have expressed the action of the kinetic energy operator on the wave function by the Fourier transform method [27], and employed the Lanczos algorithm [28] in solving the coupled equations. The time propagation has been performed in the range of 32 200 a.u.

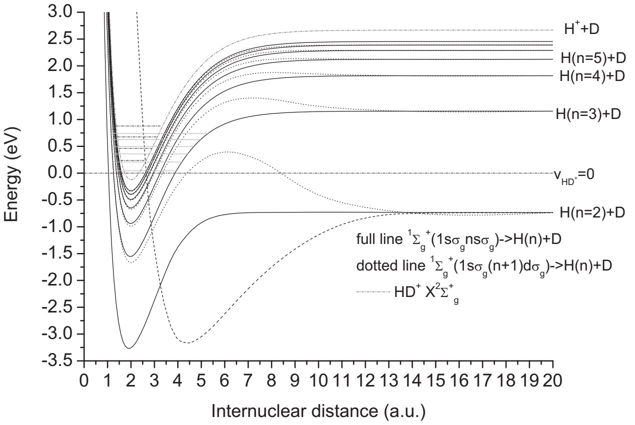

FIG. 1. The electronic states involved in the calculation: $(1s\sigma_g)$ $X^2\Sigma_g^+$ HD$^+$ ground state—black long-dashed. $(2p\sigma_u)^2$ $^1\Sigma_g^+$ HD valence state—black-dashed. $(1s\sigma_g ns\sigma_g)$ and $(1s\sigma_g(n+1)d\sigma_g)$ $^1\Sigma_g^+$ HD Rydberg states correlated with $H(n)+D$ atomic limits: full and dotted lines, respectively.

(atomic units) with the time step of 1 a.u.. As for the spatial grid, 65 536 mesh points were used. In order to avoid, as much as possible, reflections at large values of R, we have augmented the potentials of the Rydberg and of the valence states with an imaginary part $-iW$ [29,30],

$$W(R) = \alpha(R - R_{max})^3 \quad \text{if } R > R_{abs},$$

$$W(R) = 0 \quad \text{if } R \leq R_{abs}, \tag{6}$$

where $\alpha = 7.4 \times 10^{-5}$ a.u., $R_{max} = 1500$ a.u. is the value at the edge of the grid, and the threshold for flux absorption range is set $R_{abs} = 1470$ a.u..

III. RESULTS AND DISCUSSION

Figure 2 displays the cross section of DR into the valence state $(2p\sigma_u)^2$ $^1\Sigma_g^+$ in the energy range between 1.0 and 1.3 eV. The cross section curve consists of contributions from two different mechanisms [11]. The background part corresponds to what is called the *direct* mechanism (case when all the closed channels are excluded). Meanwhile, the direct process competes with the *indirect* one, based on the temporary capture into the *closed* Rydberg states labeled by their relevant quantum numbers in Fig. 2 and exhibiting characteristic resonant behavior—mostly the Fano profiles—in the shape of the cross section.

The resonances displayed and labeled in Fig. 2 superpose with other oscillations of smaller size. These originate from the fact that a wave packet trapped in a Rydberg state remains for a long time in the interaction region, and eventually arrives in the asymptotic zone very slowly. Thus the propagation time should be large enough in order for the system to have the possibility to fully react. This analysis is confirmed in a consecutive set of calculations where the amplitudes of the physical resonances increase, while those of the oscillatory remains of finite propagation converge with time to zero.

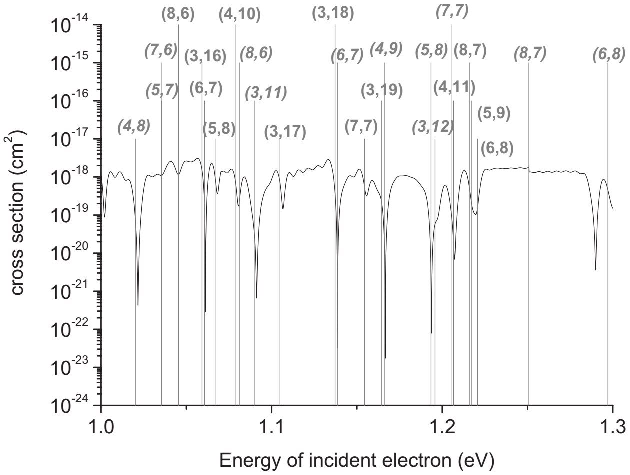

FIG. 2. Identification of resonances in the dissociative recombination into the valence state. The numbers in brackets stand respectively for the vibrational and principal quantum numbers of the Rydberg capture states. Italic characters are used for the resonances associated to $^1\Sigma_g^+$ $(1s\sigma_g nd\sigma_g)$ series, in order to distinguish them from those associated to the $^1\Sigma_g^+$ $(1s\sigma_g ns\sigma_g)$ series.

An important feature efficiently described by the present wave-packet approach, unlike from the conventional MQDT, is the opening of Rydberg states to dissociation as energy increases. Indeed, the wave packet propagates on *all* energy curves, whether valence or Rydberg, and each time a new Rydberg dissociation threshold opens, a part of the probability flux reaches the asymptotic region and contributes to the total DR cross section. This is illustrated in Fig. 3, where the valence state $(2p\sigma_u)^2$ is open already at zero energy of the incident electron, while $1s\sigma_g 4d\sigma_g$ and $1s\sigma_g 5d\sigma_g$ start to contribute at 1.15 and 1.82 eV, respectively, being resonant states of the electron capture at lower energies.

The main result of this study is displayed in Fig. 4 (black line). The cross section coming from the sum of contributions corresponding to all the open dissociative channels, is in overall good agreement with the MQDT values (gray

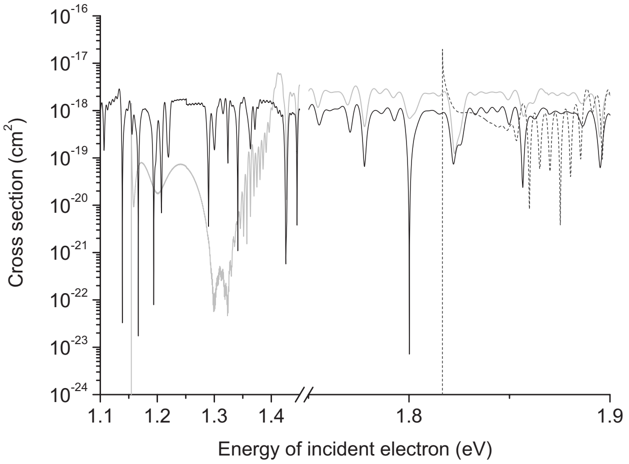

FIG. 3. State opening to dissociation: valence state $(2p\sigma_u)^2$ (black), $(1s\sigma_g 4d\sigma_g)$ (gray), $(1s\sigma_g 5d\sigma_g)$ (dashed).

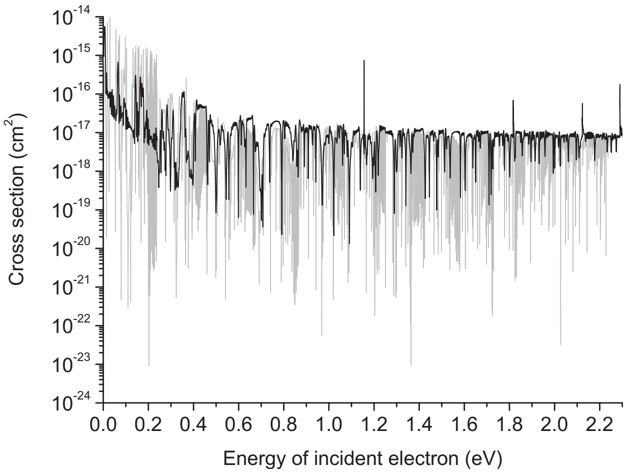

FIG. 4. DR cross section results: Wave packet (black line) vs MQDT [16] (gray line).

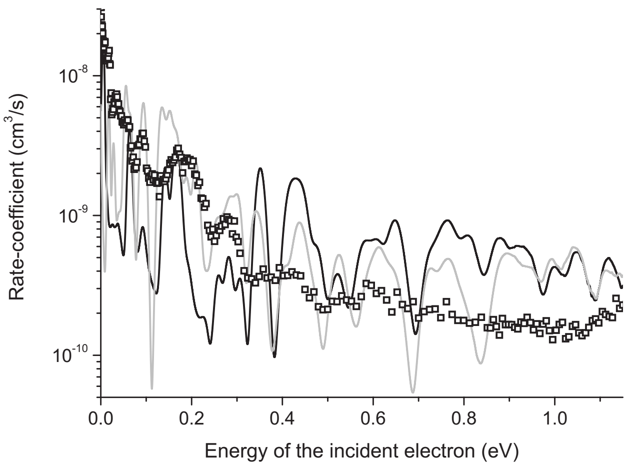

FIG. 5. DR rate coefficient results: Wave packet (black line), MQDT [16] (gray line), and the TSR experiment [7] (squares).

line). Local differences in the result are due to different nature of the two approaches. At very low energy (i.e., below 200 meV), the MQDT resonances are much more numerous and display a larger amplitude than the wave-packet ones. Indeed, one of the major strengths of the MQDT is the use of an infinite (continuous) basis set in order to describe each ionization channel, including the closed ones—responsible for the Rydberg captures [10]. Consequently, within this method, *all* the Rydberg states of capture are taken into account. As for the wave-packet approach, the number of Rydberg states is always *limited* (13 in the present case), which makes the resonant structure less rich. This explanation for the differences between the two cross sections is supported by the sensible increase of the agreement at higher energies, where the number of closed channels is rapidly decreasing and the two results become remarkably closer. Adding more Rydberg states within the wave-packet treatment will certainly act in favor of the convergence of the two theoretical cross sections. This may be a subject for further research in the near future, after the present study, which aims to *demonstrate* the applicability and potential efficiency of the wave-packet technique in the low-energy range.

Further extentions (in terms of analytical work, numerical developments, and computation time) shall include rotational effects—states and interactions—deliberately omitted in the present work. It was already demonstrated in previous MQDT studies [15,16,31] that the account of these effects is quite necessary in order to fully model and understand the experimental results. However, we believe that it is justified, even in this stage of our work, to compare theory to experiment. This is performed in Fig. 5, where the "local" rate coefficient, measured in the TSR storage ring (squares, [7]), is displayed together with the theoretical rate coefficients (black and grey lines) coming from the convolution of the cross sections from Fig. 4 with the Maxwell anisotropic distribution function characterizing the electron beam, corresponding to longitudinal and transversal temperatures of 2 and 0.1 meV, respectively. Although the result of the present calculations differs from the measured data (except of good agreement in overall trend and shape), we emphasize that the overall differences are not larger than in the case of rotation-omitted MQDT treatment, and they should diminish seriously when these latter effects will be included. Finally, one should notice the high degree of similarity between the theoretical rates coming from the convoluted MQDT and wave-packet cross sections, which is expected to evolve to convergence, when more Rydberg states will be involved in the latter.

We conclude here by recognizing the major breakthrough of this work, i.e., the emergence of resonant cross section structures (cf. Figs. 2–5) accurately describing temporary electron capture into bound Rydberg states (the indirect DR process) from the *time-dependent* calculation of dissociative recombination. The numerical effort required in the present approach is considerably higher (in terms of memory and time) than the one necessary in the MQDT approach. However, once the indirect process is taken into account, the wave-packet method is capable of providing accurate low-energy branching ratios, an information unaccessible within a pure MQDT treatment. Furthermore, the present time-dependent framework allows a straightforward extension to the dissociative recombination of polyatomic systems, which is certainly a major theoretical advantage with respect to any time-independent formalism.

ACKNOWLEDGMENTS

The authors thank Professor A. Suzor-Weiner, Professor A. Wolf, Dr. G. Moebs, and Dr. E. Charron for useful discussions, as well as F. O. Waffeu Tamo for assistance on the MQDT and computational aspects, and acknowledge financial support from CPER, CRIHAN, CNRS (PCMI, GdR "Cataplasme" and "ARCHES"), JSPS, RIKEN, and Max Planck Society. A. E. Orel also acknowledges support by NSF Grant No. PHY-05-55401.

[1] A. Wolf, L. Lammich, and P. Schmelcher (Eds.), J. Phys.: Conf. Ser. **4** (2005).
[2] S. Krohn *et al.*, Phys. Rev. Lett. **86**, 4005 (2001).
[3] L. Lammich *et al.*, Phys. Rev. Lett. **91**, 143201 (2003).
[4] V. Kokoouline and C. H. Greene, Phys. Rev. Lett. **90**, 133201 (2003).
[5] W. Geppert *et al.*, Phys. Rev. Lett. **93**, 153201 (2004).
[6] H. Kreckel *et al.*, Phys. Rev. Lett. **95**, 263201 (2005).
[7] A. Al-Khalili *et al.*, Phys. Rev. A **68**, 042702 (2003).
[8] T. Tanabe, I. Katayama, N. Inoue, K. Chida, Y. Arakaki, T. Watanabe, M. Yochizawa, S. Ohtani, and K. Noda, Phys. Rev. Lett. **70**, 422 (1993).
[9] A. I. Florescu-Mitchell and J. B. A. Mitchell, Phys. Rep. **430**, 277 (2006).
[10] Ch. Jungen, *Molecular Applications of Quantum Defect Theory* (Institute of Physics Publishing, Bristol, 1996).
[11] A. Giusti-Suzor, J. Phys. B **13**, 3867 (1980).
[12] A. Giusti-Suzor, J. N. Bardsley, and C. Derkits, Phys. Rev. A **28**, 682 (1983).
[13] S. L. Guberman and A. Giusti-Suzor, J. Chem. Phys. **95**, 2602 (1991).
[14] I. F. Schneider, O. Dulieu, and A. Guisti Suzor, J. Phys. B **24**, L289 (1991).
[15] H. Takagi, J. Phys. B **26**, 4815 (1993).
[16] I. F. Schneider, C. Strömholm, L. Carata, X. Urbain, M. Larsson, and A. Suzor-Weiner, J. Phys. B **30**, 2687 (1997).
[17] H. Takagi, Phys. Rev. A **70**, 022709 (2004).
[18] S. L. Guberman, Phys. Rev. A **49**, R4277 (1994).
[19] V. Kokoouline and C. H. Greene, Phys. Rev. A **72**, 022712 (2005).
[20] B. K. Sarpal, J. Tennyson, and L. A. Morgan, J. Phys. B **24**, 1851 (1994).
[21] A. E. Orel, Phys. Rev. A **62**, 020701 (2000).
[22] I. F. Schneider, A. E. Orel, and A. Suzor-Weiner, Phys. Rev. Lett. **85**, 3785 (2000).
[23] A. Larson and A. E. Orel, Phys. Rev. A **64**, 062701 (2001).
[24] F. Texier and Ch. Jungen, Phys. Rev. A **59**, 412 (1999).
[25] D. T. Birtwistle and A. Herzenberg, J. Phys. B **4**, 53 (1971).
[26] C. W. McCurdy and J. L. Turner, J. Chem. Phys. **78**, 6773 (1983).
[27] D. Kosloff and R. Kosloff, J. Comput. Phys. **52**, 35 (1983).
[28] C. Leforestier *et al.*, J. Comput. Phys. **94**, 59 (1991).
[29] C. Leforestier and R. E. Wyatt, J. Chem. Phys. **78**, 2334 (1983).
[30] D. Neuhauser and M. Baer, J. Chem. Phys. **90**, 4351 (1989).
[31] T. Tanabe *et al.*, Phys. Rev. Lett. **75**, 1066 (1995).